16th World Conference on Earthquake, 16WCEE 2017

Santiago Chile, January 9th to 13th 2017

Paper N° 671

Registration Code: S-O1462843162

SHAKE TABLE TESTS ON 1100 kV GIS BUSHING-SUPPORT FRAME SYSTEMS

C. He(1), Q. Xie(2), G.L. Ma(3)

(1) *Shanghai, China, Department of structural engineering, Tongji University, cc.he@foxmail.com*
(2) *Shanghai, China, Department of structural engineering, Tongji University, qxie@tongji.edu.cn*
(3) *Shanghai, China, Department of structural engineering, Tongji University, mgldut@163.com*

Abstract

With the increase of the voltage, the substation equipment usually made of porcelain is more vulnerable subjected to severe earthquakes. In order to evaluate the seismic performance of the ultra-high voltage (UHV) gas insulated switchgear (GIS) bushing-support frame system, in this paper, shake table tests on a full-scale 1100kV GIS bushing with real support frame and canister for electrical device for alternating current (AC) was carried out. At the critical parts of the system, the dynamic responses were measured. The results indicate that the dynamic properties of the system were changed obviously under different levels of input ground motion with peak ground accelerations less than 0.15g. After retrofitting the frame, the system was retested under the input ground motion of which peak ground acceleration (PGA) is 0.4g and the dynamic properties of the system changed slightly. There wasn't any visible mechanical damage to the bushing. The damping ratio of the bushing-support frame system is small and the amplification factors of the supporting frame is larger than that specified in relevant specifications.

Keywords: seismic performance; shake table test; 1100 kV GIS bushing

1. Introduction

Substations are important components in electrical lifeline systems and the electrical equipment is the key point in substations. Once the electrical equipment are damaged during the earthquake, there will be a huge economic loss directly or indirectly and the electricity interruption may make it difficult in disaster relief and rebuilding.

The electrical equipment such as circuit breakers, disconnecting switches, transformers and arresters are independent and they are connected by bus. In order to improve the degree of reliability of the circuits and to simplify the design of substations, the electrical equipment listed above was installed in metal tube which was filled with the insulating gas (SF_6). The combination unit is called as gas insulated switchgears (GIS). The bushing installed on a GIS is called as GIS bushing. The GIS used in substations are showed in Figure 1.

Fig. 1 – GIS used in substation

In the past years, the earthquake had severely destroyed substations systems, such as the Kocaeli earthquake in Turkey in 1999 [1]. About the equipment such as disconnecting switches and arresters, the earthquake also engendered severe destruction on them. In China, the disconnecting switch damaged in Tangshan earthquake accounted for 30% [2]. In 2008, the Wenchuan earthquake destroyed 40 disconnecting switches of which the voltage were above 252 kV [3]. The construction of GIS bushing is similar with disconnecting switch or arrester, which means they have the same failure features. Due to the fragility of porcelain material which is utilized to manufacture the bushings, the narrow slender GIS bushing is vulnerable subjected to earthquake. So the seismic performance of GIS bushing is important in earthquake region such as China. Before the manufacture win the bidding, the seismic performance of the bushing should be evaluated and the seismic response must meet Chinese standards.

There are many researches about the seismic performance of electrical equipment. In 2007， Whittaker et al. had seismic evaluation and analysis of high-voltage substation disconnecting switches. They found the vulnerable components of the switches were the post-blade connections at the base of the posts [4]. In 2012, Mohammadi et al. calculated the dynamic properties of substation support structures. The formula to estimate the amplification factor of the frame was listed in this paper [5]. In 2013， Koliou et al. found the flexural stiffeners have an influence on the amplification factor of transformer tanks by a numerical study [6]. Due to the different design between different manufacturers and the complex structure of the GIS, the research on the seismic performance for the GIS or their bushing is difficult. In 1993, Buck et al. tested the seismic performance of a typical 170 kV two-span GIS and analyzed it by a finite element method (FEM). The results showed that the GIS could withstand earthquake of which the PGA was 0.75 g (g is the unit of gravitational acceleration) [7]. In 2013, Lin et al. obtained the seismic response of a 1100 kV UHV GIS by FEM. Different time histories was used and the results showed that the safety factors were larger than the value recommended by standards [8]. Liu et al. did shake table tests and FEM analysis on a GIS of which type is ZF22-126. The results of the research indicated that the seismic performance of GIS could be used at high seismic intensity area [9].

With the increase of the voltage, the bushings for 1100 kV UHV GIS are taller and slenderer than the equipment running in lower voltage, which makes bushings more vulnerable during in disaster. Due to the complex structure of GIS bushings and the difficulties to ensure the stiffness of flange, it is necessary to take the shake table tests to evaluate the seismic performance of 1100 kV UHV GIS bushing. In this paper, shake table tests were carried out on a full scale GIS bushing with two different frames and the seismic performance of the bushing was evaluated.

2. Description of test specimen

2.1 GIS bushings and canister

The overall length of the bushing is 12.02 m. For the bushing, the inner and the outer diameter at the top section is 400 mm and 470 mm, respectively. The diameter at the bottom section is 860 mm and 960 mm, respectively. The bushing contains 10 porcelain units, a cupreous flange and a metallic grading ring at the top of the bushing. The connections between flange and the neighboring porcelain unit or between different adjacent porcelain segments are made by adhesive material. The porcelain part protects and supports the bus and electric device in the bushing. Meanwhile, the grading ring is installed to maintain the stability of electromagnetic field. Also, the bushing is installed on the frame by the connection of a flange. A central conductor of which the material is aluminum run through the porcelain bushing. The central conductor is longer than the porcelain part and the electric current is transmitted by the conductor. The central conductor connect the device which is installed in a metallic canister below the bushing. In the porcelain bushing, the shielding ring was used also for the stability of the electromagnetic field. The length of the metallic canister which is made by steel is about 4 m. To withstand the temperature stress and deformation, the metallic canister is divided into 3 parts and they are connected by flexible corrugated pipe. The bushing and the canister was filled with insulating gas (SF_6), so the equipment like disconnecting switches or surge arresters could be installed in the metallic tube, as Figure 1 shows, which could reduce the cost of the equipment. The total weight of the porcelain bushing is about 8000 kg and the weight of the grading ring which is made by aluminum, a metallic material of which the density is small, is 90 kg. The total weight of the canister is 1010 kg. The shape and dimensions of the GIS bushing is showing in Figure 2.

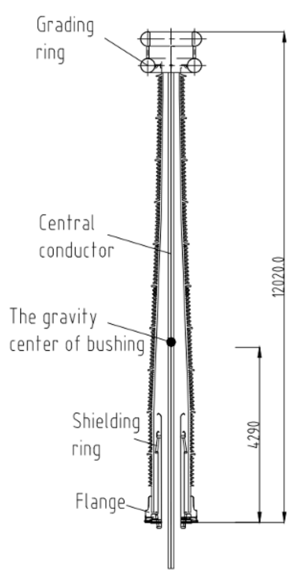

Fig. 2 – Shape and dimensions of 1100 kV GIS bushing

2.2 Supporting frame

Due to the volume of the electric device, the metallic tube, the construction of the bushing and the canister, a supporting frame is needed to install the electric equipment. There were two full-scale supporting frames used for the bushing in this paper. The first one of them was supplied by the sponsor for test. After the test, the sponsor supplied another frame with the same type but had taken some retrofitting measures. In this paper, the two frame were named as Frame-O and Frame-R, respectively.

Steel was used to build the supporting frame. The columns of the supporting frame were made by wide flange H profiled bar (H 300×300×10×15 mm). In the main vibration direction, there were braces between columns and the braces were made by angle (L 100×100×10×10 mm). In another direction of the supporting frame, beams were installed and the section of beam is same with columns. Because the metallic canister should be installed below the frame cover plate and between the columns of the frame, the supporting frame have dimensions of 2000×2000 mm at the bottom and the top. What's more, the height of the supporting frame was 5870 mm, which was design to accommodate the canister. The thickness of the cover plate on the supporting frame is 40 mm. A hole of which the diameter is 960 mm had been set through the cover plate to fix the bushing and the bushing was fixed on the frame by the flange.

The connections or the joints between beams and columns or braces and columns for the frame are bolted connections. For the convenience of the installation, the bolt holes is long and the bolt could slip in them, so the requirements for the installation accuracy cold be lower and the supporting frame could be assembled in site. However, for the lack of the knowledge of structure mechanics, the manufacturer ignored the construction measures about the joints. The joints of beams and columns are showed in Figure 3 (a). There is only one ear plate connected the flange of column and beam, so the beams can't tie the columns fasten and lateral stiffness of the supporting frame is small, which may have negative impact on the porcelain bushing according to reference [5]. Between the flanges of the joints, there is no stiffeners, so the load transfer path is incomplete. The force from the beam can't transfer to the column directly. During the test, there were some problems about the frame, so the supporting frame was retrofitted after the test and retrofit measures will be introduced in the next section.

2.3 Retrofit measures

The dynamic characteristics have a great influence on the seismic response of the bushing [5]. In order to improve the seismic performance of the UHV GIS bushing, 3 available measures were taken by the manufacturer at the supporting frame. What's more, the 3 measures are convenient to carry out in site, so the frames which are in service could be retrofitted and the requirements for installation accuracy are not improved.

Firstly, the number of ear plate at the joints of beams and columns were increased. The stiffness of the joints increased and the lateral stiffness of the supporting frame increased. Secondly, the stiffeners at the joints was assembled, the force from beams or braces could transfer to columns directly and the local buckling of web or flange was suppressed. Finally, in the main vibration, the horizontal braces were assembled. In another direction, the braces were installed between beams. Figure 3 (b) presents the layout of the ear plates and stiffeners in Frame-R.

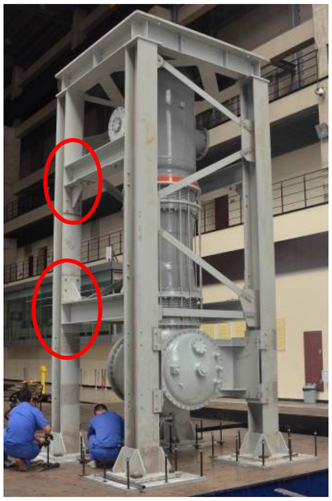

(a) The construction of Frame-O

(b) The construction of Frame-R

Fig. 3 – Supporting frames and the joints of beams and columns

3. Experimental program

3.1 Earthquake time history

To evaluate the seismic performance of the bushing, an artificial earthquake time history, normalized to a peak acceleration of 1.0 g, showed in Figure 4 (a) was used. This artificial time history was modified from the record of Landers in 1992 to the Chinese standard [10]. The required response spectra (RRS) of the Chinese standard is presented in Figure 4 (b). The plateau of the RRS start at 0.1 s and stop at 0.9 s. If the site predominant period (T_g) is known, the 0.9 s could be changed to a smaller one. When T_g is set as 0.9 s, it means the RRS could envelope four classes of site in China.

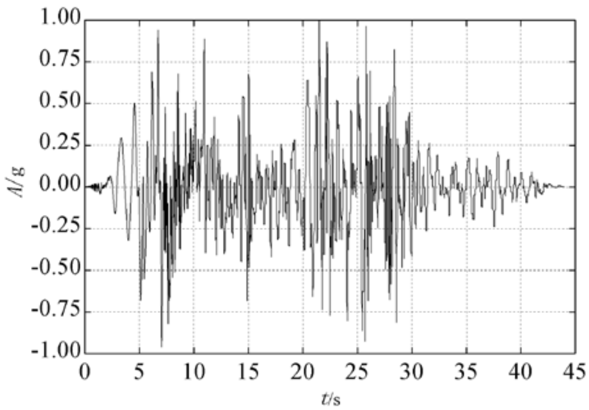

(a) The time history of artificial wave

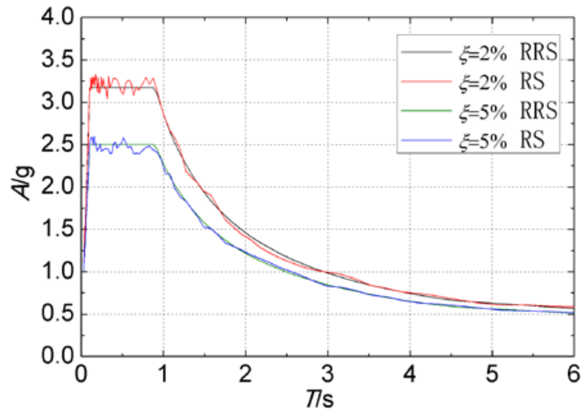

(b) The comparison of RRS and response spectra (RS) of artificial wave

Fig. 4 – Time history and response spectra of the artificial wave

Due to the control of the oil pump and the displacement limitation of shake table, the table response spectra (TRS) had some difference with the RRS. In the tests for GIS bushing, the high-pass filters were used and the filter points of the tests were 0.2 Hz. When PGA of the tests were 0.4 g and the damping ratio was 2%, the TRS for bushing with Frame-R could be found in Figure 5. The earthquake wave was input to the shake table uniaxially and the main vibration direction is called as X in this paper.

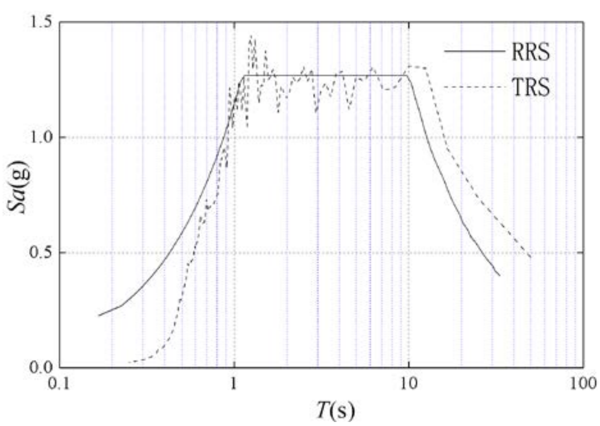

Fig. 5 – TRS and RRS for GIS bushing with Frame-R

3.2 Working conditions of tests

Table 1 and Table 2 summary the test conditions (TC) of the 2 tests with different supporting frames. The white noise was used for identifying the dynamic characteristics before the tests and for detecting whether there was any structure damage after the shake table tests. The destinations of TC 2, TC 3 and TC 4 for bushing with Frame-O or Frame-R were to optimize the table parameters and to minimize the tolerance between TRS and RRS. For some reasons which will be introduced in the following segments, the bushing with Frame-O couldn't be excited by the artificial time history of which the PGA is 0.4 g. TC 6 and TC 8 for bushing with Frame-R were carried out to evaluate the seismic performance of the GIS bushing. The installation of UHV GIS bushing with Frame-O is showed in Figure 6.

Table 1 – The test condition for bushing with Frame-O

Test	**Test condition**	
	Earthquake wave	**Target PGA / g**
TC 1	White noise	0.075
TC 2 / TC 3 / TC 4	Artificial wave	0.15
TC 5	White noise	0.075

Table 2 –The test condition for bushing with Frame-R

Test	**Test condition**	
	Earthquake wave	**Target PGA / g**
TC 1	White noise	0.075
TC 2 / TC 3 / TC 4	Artificial wave	0.15
TC 5	White noise	0.075
TC 6	Artificial wave	0.20
TC 7	White noise	0.075
TC 8	Artificial wave	0.40
TC 9	White noise	0.075

3.3 Test point arrangement

To obtain the dynamic characteristics of the bushing-support systems, accelerometers were arranged along the longitude of the bushing and frames. At the tests of the bushing with Frame-O, 11 accelerometers were used and at the test of GIS bushing with another frame, the number of accelerators were 15. The arrangement of accelerometers along the bushing with Frame-R is presented in Figure 7.

What the manufacturer concerned about was the stress in the porcelain bushings. From the damage in past earthquakes and the dynamic characteristic of cantilever beam, many bushings cracked at the bottom sections, so strain gauges were used at the bottom section of bushings and the connection sections which were between the adjacent porcelain units of bushing. For GIS bushing, 8 strain gauges were arranged at the bottom section for the test and all the strain gauges were arranged in the longitude direction of the bushing.

Fig. 6 – The installation of the specimen in laboratory

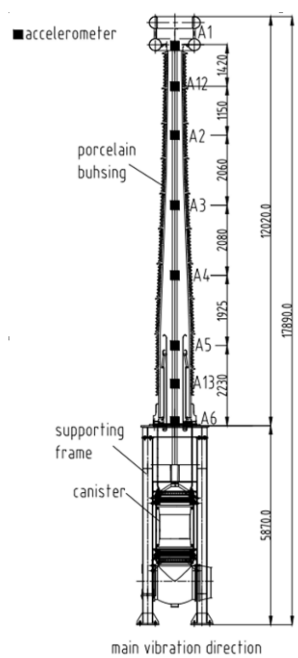

Fig. 7 – Test points arrangement of GIS bushing with Frame-R

4. Experimental results

4.1 Dynamic characteristics

Before the installation of the equipment, the hammering tests were carried out on the frames to estimate the fundamental frequency of the frames. Figure 8 is the Fourier spectrum of the two frames, the fundamental frequency of Frame-O and Frame-R was 7.35 Hz and 8.62 Hz, respectively. The retrofit of the joints and braces increase the frequency of the Frame. However, the fundamental frequency of the two bushing was in the plateau of the RRS, which means the amplification effects for the bushing of the two frames will be violent.

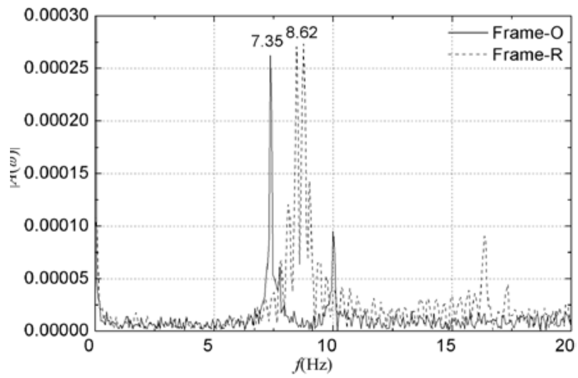

Fig. 8 – The Fourier spectrum of the two frames

Table 3 presents the frequencies and damping ratios of the UHV GIS bushing with two different frames. Because of the optimization of the joints and the lateral resistant system, the frequencies and the damping ratio of bushing with Frame-R were higher than bushing with Frame-O obviously.

Table 3 - The dynamic properties of the bushing with two different frames

Bushing	Fundamental frequency (Hz)	Second order frequency (Hz)	Damping ratio
Bushing-O	2.75	7.375	0.49%
Bushing-R	3.125	11.125	1.06%

4.2 Evaluation of bushing with non-retrofitted frame

Definite amplification factor as the ratio between the peak acceleration at the top of the frame and the PGA. For bushing with Frame-O, the amplification factors in TC 2 to TC 4 were listed in Figure 9. The amplification factors became bigger and bigger with the number of tests increased. According to the elastic theory, the response of a structure is proportional to the load. From what has been discussed above, what can be referred was the stiffness of the frame had changed during the tests, so the seismic performance evaluation of the bushing stopped and the frame does not apply in seismic area.

4.3 Evaluation of bushing with retrofitted frame

After the retrofit of frame, the GIS bushing was tested again. Figure 10 is the transfer function of TC 1, TC 5, TC 7 and TC 9. Before and after tests, the fundamental frequency and the second order frequency decreased from 3.125 Hz to 3.000Hz and from 11.125Hz to 10.625 Hz, respectively, which means the dynamic characteristic of the system changed slightly. From the comparison of the four lines, the shape of the curves were very similar and from the phenomenon in laboratory, which can be inferred was the bolts looseness and the bolts slip in the holes lead to the decrease of the frequencies. For the engineering application of the frame, the long holes should be replaced and the high-strength bolts should be used to raise the stiffness of the frame.

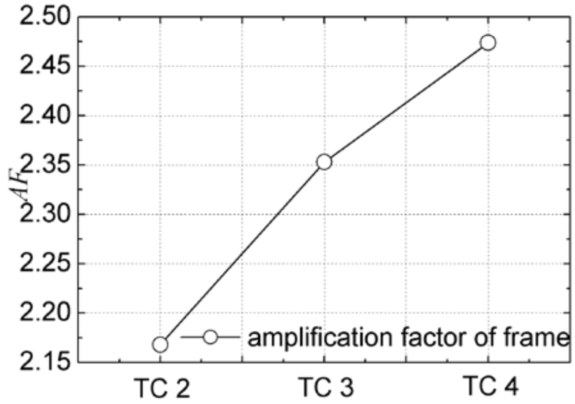

Fig. 9 – Amplification factors of TC 2 to TC 4

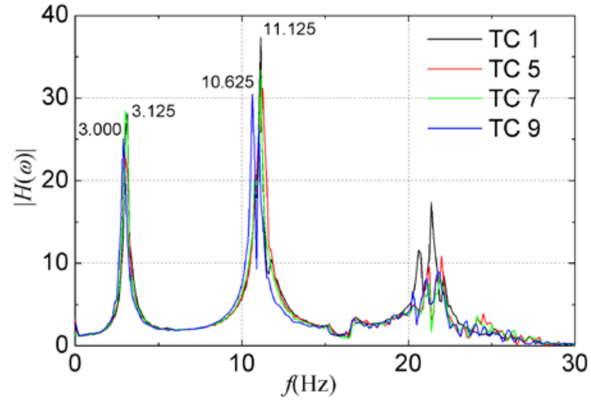

Fig. 10 – Transfer function of GIS bushing-support system

According to the data provided from the manufacturer, the Young's module and the ultimate strength of porcelain material is 100 GPa and 45 MPa, respectively. What the manufacturer concerned about was the stress of the porcelain. Figure 11 is the strain in the main vibration direction at the bottom section of the porcelain bushing in TC 8. Table 4 lists the maximum tensile and compressive stress along the longitude direction of the bushing at the main vibration direction of different test conditions. The maximum tensile strain and the maximum pressure strain in TC 8 around bottom section are showed in Figure 12. From this picture, the maximum stress were symmetric roughly about the main vibration direction. The maximum stress in TC 8 could be obtained and the corresponding value was 6.83 MPa, which means there was no damage in the porcelain material. The conclusion was in accordance with the phenomenon observed in the laboratory.

Table 4 The stress of bushing with Frame-R (Unit: MPa)

Stress	**TC 4**	**TC 6**	**TC 8**
Tensile stress	3.18	3.89	6.48
Compressive stress	2.60	3.61	7.17

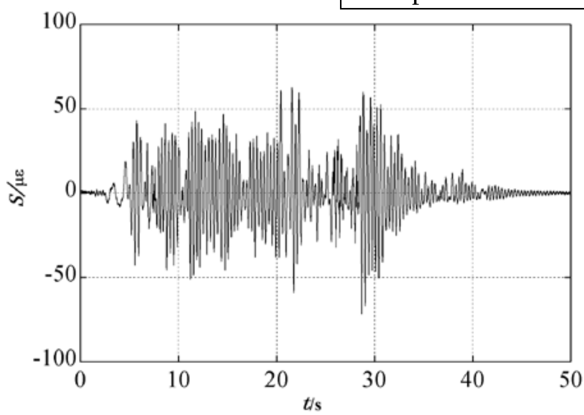

Fig. 11 – Strain in main vibration direction at the bottom section of TC 8

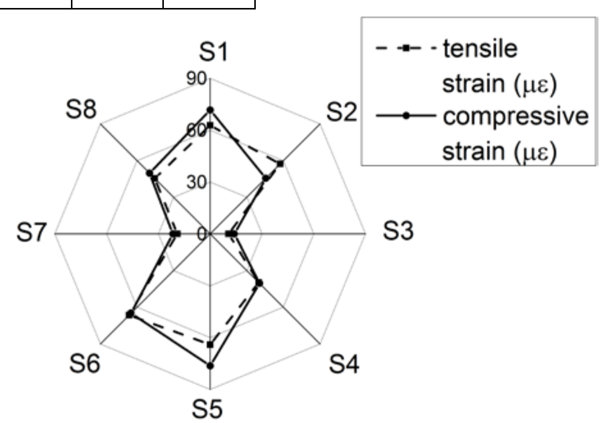

Fig. 12 – The maximum tensile and compressive strain at the bottom section of TC 8

The displacements about the bushing were important parameters to evaluate the seismic performance of the equipment. On the one hand, due to the influence of electromagnetic field, the redundancy of the bus shouldn't exceed the limiting value, so there will be tension force in the flexible bus which is connected with the equipment when the displacement of the equipment is large enough. The equipment may even be damaged by the tension force in the flexible bus [11]. The displacement at the top of the bushing wasn't measured since the height of bushing resulted in the difficulties in the arrangement of displacement meters. The displacements at the top of the bushing were calculated by the quadratic integration of the acceleration in frequency domain. The displacement at the top of UHV GIS bushing with Frame-R in X direction was presented in Figure 13. The maximum deflection was 66.0 mm at the top of the bushing. The interaction between the equipment and the flexible bus could be avoid after a scientific design.

Define the bushing amplification factor (BAF) as the ratio of peak acceleration at different height along the bushing and the peak acceleration of the shake table. In different test conditions of the GIS bushing with Frame-R, the BAF was showed in Figure 14. What can be concluded from Figure 14 was the amplification factors of frame and bushing were larger than 2 and frame amplified the seismic response of the GIS bushing and the phenomenon indicated that the frame should be optimized. In most cases, with the increase of PGA, the BAF get smaller.

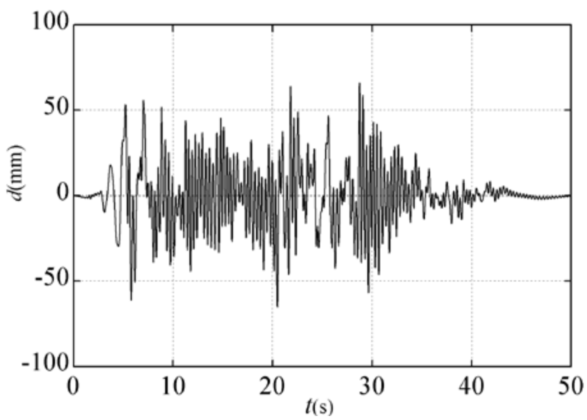

Fig. 13 – The top displacement of the bushing with Frame-R of TC 8

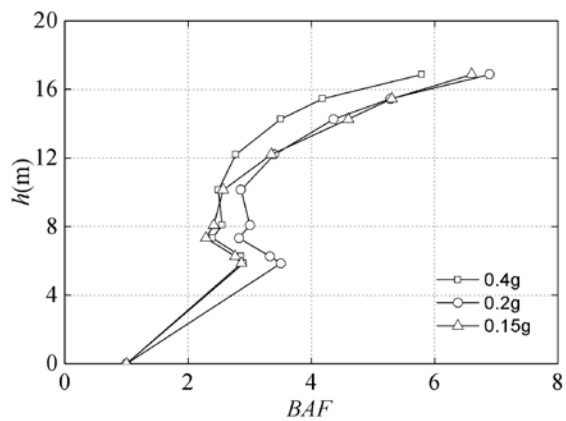

Fig. 14 – The BAF of the bushing with Frame-R in different test conditions

5. Comparison and discussion

TC 4 for the bushing with different frames were the most close to the target spectra after the iteration and the PGA for the two test conditions were the same, so the response of the bushing with two frames in TC 4 was compared.

The acceleration distribution along bushing-support systems reflected the dynamic properties of the equipment. The BAF of the bushing with two different frames are showed in Figure 15. The line with circle symbols respects the BAF of the GIS bushing with Frame-R and the BAF was much smaller than the BAF of bushing with Frame-O, represented by the line with square symbols. The reinforcement of frame could increase the stiffness of the bushing-support system and reduce the acceleration response of the bushing. Another conclusion could be drew from Figure 15 is with the increase of the height of test points, the response of acceleration increased nonlinearity. From the curvature of the two lines, the stiffness of the bottom part of the bushing is much larger than the stiffness of two frames.

In Chinese code for seismic design of electrical installations [10], the amplification factors of frame should be smaller than 1.4. As Figure 15 shows, in the tests of the GIS bushing, the amplification factors for bushing with Frame-O and Frame-R were 2.46 and 2.87 respectively. Both of them were much larger than the value that specified in relevant specifications.

The strain of the bushing in two different conditions are presented in Figure 16. For the comparison of the two lines in Figure 15 and Figure 16, what could be concluded is that the dynamic properties of the frame have a great influence of the system. The acceleration and the strain response of the bushing with Frame-O was much larger than the bushing with another frame. In Chinese code and in IEEE standard [12], the amplification factor of the supporting frame was used to evaluate the influence of the frame on the seismic performance of the system. However, the amplification factor of Frame-R was larger Frame-O, but the response of bushing with

Frame-R was much smaller than the bushing with Frame-O. For the elaborate analysis of the influence of supporting frame on the seismic performance of the system, according to the reference [5], the mass distribution and the stiffness distribution or even the frequency spectrum characteristics of the earthquake time history should be concerned.

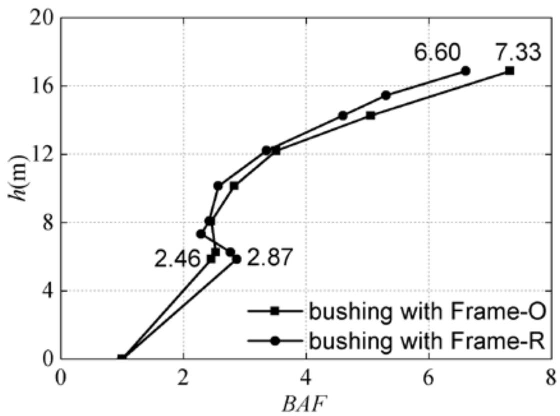

Fig. 15 – The BAF of GIS bushing with two different frames

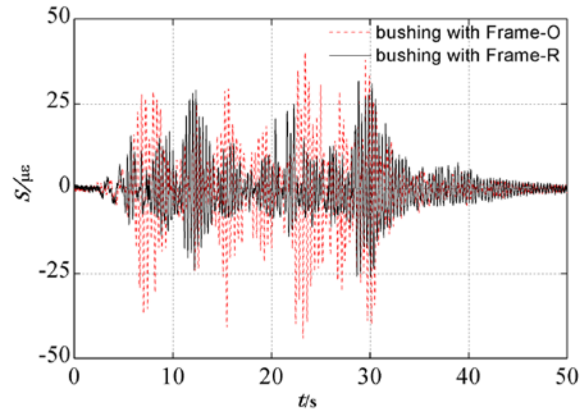

Fig. 16 – The comparison of the strain response of the two bushing with different frames

6. Conclusion

The seismic performance of 1100 kV UHV GIS bushing with original supporting frame and with retrofitted frame was evaluated. The key conclusions of the tests are presented below.

1. Before the retrofitting of the frame, the stiffness of the frame changed and it does not apply in seismic area.

2. After retrofitting, the bushing was able to sustain the inertia force caused by the earthquake and the dynamic properties did not change obviously after tests. Comparing with the bushing with Frame-O, the type of bushing with Frame-R was more appropriate for highly intensive seismic region.

3. Although the bushing with retrofitted frame survived during the earthquake, the amplification factor of the frame was larger than the value recommended in standards. The construction and the stiffness of the supporting frame should be improved.

4. After retrofitting, the stiffness of the frame and the system was increased and main dynamic response of bushing with Frame-R was decreased comparing with bushing with Frame-O.

5. The construction and the stiffness of the frame has a great influence on the bushing-support system. For the engineering application of the GIS bushing, the dynamic characteristics of Frame-R should be optimized.

7. Acknowledgements

The tests described in this paper were carried out by Tongji University with the funding from State Grid Corporation of China (SGCC). The authors wish to thank the following people for the contributions to the tests: Mr. Yang of the College of Civil Engineering; Mr. Zhang, Mr. Wu of the shake table laboratory and Mr. Sun of SGCC.

8. References

[1] AIJ, JSCE, JGS (2001): *Report on the damage investigation of the Kocaeli earthquake in Turkey*. Maruse Press.

[2] Li YQ, Li XJ, Liu XH (2002): A summary on the seismic analysis in the electrical system. *World Earthquake Engineering*, **18** (4), 79-81.

[3] Yu YQ, Li GF, Li P (2008): Investigation and analysis of electric equipment damage in Sichuan power grid caused by Wenchuan earthquake. *Power System Technology*, **32** (11), 5-10.

[4] Whittaker AS, Febves GL, Gilani ASJ (2007): Seismic evaluation and analysis of high-voltage substation disconnect switches. *Engineering Structures*, **29**, 3538-3549.

[5] Mohammadi RK, Akrami V, Nikfar F (2012): Dynamic properties of substation support structures. *Journal of Constructional Steel Reasearch*, **78**, 173-185.

[6] Koliou MK, Filiatrault A, Reinhorn AM (2013): Seismic response of high-voltage tramsformer-bushing systems incorporating flexural stiffeners I: numerical study. *Earthquake Spectral*, **29** (4), 1335-1352.

[7] Buck KE, Tebbe AK, Rees V (1993): Verification of the seismic resistance of gas-insulated switchgear (GIS). *IEEE Transaction on Power Delivery*, **8** (1), 114-120.

[8] Liu X, Shi KJ, Xu JY (2013): Analysis on seismic performance of ultra-high voltage HGIS equipment. *Journal of Sheng yang University of Technology*, **35** (2), 121-125.

[9] Liu Y (2013): Experimental study on seismic performance of gas insulator switchgear. *Master's thesis*, Xi'an university of science and technology, Xi'an, China.

[10] MOHURD, AQSIQ (2013): Standard GB 50260, Code for seismic design of electrical installations.

[11] Xie Q, Wang YF, Zhu RY (2011): Shaking table test on real substation equipment connected by conductors with different sag. *Journal of Earthquake Engineer and Engineering Vibration*, **31** (1), 67-73.

[12] IEEE (1997): Standard No. 693, Seismic qualification recommendation for substation equipment.